THE SLIPPERY ROAD TO SLIDING CONTROL: CONVENTIONAL VERSUS DYNAMICAL SLIDING MODE CONTROL

MARC VAN DE WAL, BRAM DE JAGER* AND FRANS VELDPAUS

Faculty of Mechanical Engineering, Eindhoven University of Technology, P.O. Box 513, 5600 MB Eindhoven, The Netherlands

SUMMARY

Theory and design of a conventional sliding mode controller (CSMC) and a dynamical sliding mode controller (DSMC) are discussed and compared. The controllers are applicable to uncertain nonlinear MIMO systems. Emphasis is put on handling of unmodelled dynamics, tuning of controller parameters, suppression of chattering, and robust tracking performance. Experiments are performed with a mechanical manipulator. Errors in the model of this manipulator are due to, amongst other things, neglected flexibilities. It is concluded that for this set-up the robustness to these model-reality differences is approximately the same for both controllers, while nominal performance is best for the CSMC. © 1998 John Wiley & Sons, Ltd.

Key words: sliding mode control; robust control; nonlinear control; experimental application

1. INTRODUCTION

Dynamic systems are controlled in order to follow a prescribed trajectory with a certain accuracy. The control is often based on a mathematical model of the system. This model is never an exact representation of reality, since modelling errors are inevitable. Moreover, one can use a simplified model on purpose. In this article, the unmodelled dynamics error is of primary interest, i.e., the error due to unmodelled modes, unmodelled actuator and sensor dynamics, neglected time delays, etc.

The erroneous model and the demand for high performance require the controller to be robust. One class of robust controllers, sliding mode controllers (SMC), is based on variable structure control, see Reference 1. These controllers can be used if the inaccuracies in the model structure are bounded with known bounds. However, an SMC has some disadvantages, related to chattering of the control input signal. Often this phenomenon is undesirable, since it causes excessive control action leading to increased wear of the actuators and to excitation of unmodelled dynamics.

This paper was recommended by publication by editor A. Sideris

* Correspondence to: Bram de Jager, Faculty of Mechanical Engineering, Eindhoven University of Technology, P.O. Box 513, 5600 MB Eindhoven, The Netherlands. E-mail: A.G. de.Jager@wfw.wtb.tue.nl

Chattering can be avoided, for instance, by the 'boundary layer modification' of Slotine and Li.[2] Unfortunately, then robustness and performance are impaired in comparison with the unmodified SMC. Another approach to avoid chattering is proposed by Bartolini,[3] Sira-Ramírez,[4] and Bartolini and Pydynowski.[5] Their idea is to use a derivative of the control law as a discontinuous forcing action. The resulting dynamical sliding mode controller (DSMC) should produce substantially smoothed input signals, at the same time maintaining the favourable features of the conventional SMC.

In this paper, the robustness to unmodelled dynamics and the performance of the conventional SMC with boundary layer modification (CSMC) and of the DSMC are investigated. Sufficient conditions for the controller gains to guarantee stability in the presence of modelling errors are developed. To avoid conservative designs, requirements for each individual input are derived. Until now, this topic has been given only limited attention in the literature. Guidelines for tuning the controllers are derived and explained. Both CSMC and DSMC are implemented as sampled data controllers in an experimental nonlinear MIMO system. To avoid offsets in the mean of the tracking error of the DSMC, the control law as proposed by Bartolini[3] is modified. Robustness in the sense of sensitivity of the closed-loop performance to modelling errors[2] is investigated and the results are compared for both controllers.

The paper has the following structure. Section 2 gives some preliminaries and fixes the notation. Section 3 and Section 4 present the CSMC and the DSMC, respectively. The robust performance of the controllers is investigated by experiments as discussed in Section 5. Finally, in Section 6 the main conclusions are drawn.

2. PRELIMINARIES

We restrict ourselves to nonlinear, affine MIMO systems. It is assumed that the controller design model is feedback linearizable, so its relative degree r equals its order n.[2] Only square systems are considered, i.e., the number m of inputs u_i equals the number of outputs y_i to be controlled.

The design model can be written in normal form as

$$y_i^{(n_i)} = \hat{f}_i(x) + \sum_{j=1}^{m} \hat{B}_{ij}(x)u_j \quad \text{for } i = 1, \dots, m \tag{1}$$

where the state vector $x \in \mathbb{R}^n$ is

$$x = \begin{bmatrix} y_1 & \dot{y}_1 & \cdots & y_1^{(n_1-1)} & \cdots & y_i & \dot{y}_i & \cdots & y_i^{(n_i-1)} & \cdots & y_m & \dot{y}_m & \cdots & y_m^{(n_m-1)} \end{bmatrix}^{\mathrm{T}}$$

and the functions $\hat{f}_i(x)$ and $\hat{B}_{ij}(x)$ are differentiable at least once. This model has vector relative degree $[n_1 \ n_2 \ \cdots \ n_m]$ and total relative degree $r = \sum_{i=1}^{m} n_i$. The assumption $r = n$ implies the absence of internal dynamics.

The real system is seen as a system of order $n^* \geqslant n$, but with the same vector relative degree. If $n^* > n$, internal dynamics plays a role in the real system. It is assumed that the internal dynamics of the real system is stable. The interesting part of this system then is described in normal form by

$$y_i^{(n_i)} = f_i(x^*) + \sum_{j=1}^{m} B_{ij}(x^*)u_j \quad \text{for } i = 1, \dots, m \tag{2}$$

$$\dot{x}' = q(x^*) + Q(x^*)u$$

where the state vector $x^* \in \mathbb{R}^{n^*}$ of the real system is

$$x^* = [x^T \ x'^T]^T; \qquad x' = [x'_{n+1} \ \cdots \ x'_{n*}]^T$$

and $f(x^*)$, $B(x^*)$ are differentiable at least once.

For compactness of notation, design model (1) and the real system (2) are written in 'controllability canonical form' as[2]

$$\text{design model: } y^{(n)} = \hat{f}(x) + \hat{B}(x)u \tag{3}$$

$$\text{real system: } y^{(n)} = f(x^*) + B(x^*)u \tag{4}$$

where the vector $y^{(n)}$ is defined by

$$y^{(n)} = [y_1^{(n_1)} \ y_2^{(n_2)} \ \cdots \ y_m^{(n_m)}]^T$$

It is assumed that the square matrix $\hat{B}(x)$ is locally regular around x.

The descriptions in (3) and (4) give rise to the definition of the following modelling errors, caused by unmodelled dynamics, parameter errors, etc.:

$$\Delta f(x^*) = f(x^*) - \hat{f}(x); \quad \Delta B(x^*) = B(x^*) - \hat{B}(x)$$

We assume that $\Delta f(x^*)$ and $\Delta B(x^*)$ are bounded with known bounds.

3. CONVENTIONAL SLIDING MODE CONTROL

The first step in CSMC-design is to define m switching co-ordinates $s_1, s_2, \ldots, s_m$ by

$$s_i = e_i^{(n_i - 1)} + e_{c_i}; \quad e_i = y_i - y_{d_i}; \quad e_{c_i} = \sum_{j=1}^{n_i - 1} \eta_{i,j} e_i^{(j-1)} \quad \text{for } i = 1, \ldots, m \tag{5}$$

with tracking error e_i, desired output y_{d_i}, and constants $\eta_{i,j}$ ($j = 1, \ldots, n_i - 1$) which are chosen such that the desired error dynamics is obtained if $s = [s_1 \ \cdots \ s_m]^T = 0$.

The idea is to determine an input u that achieves $s = 0$ in finite time from every initial error and keeps $s = 0$ afterwards. The control law proposed to achieve this is

$$u = \hat{B}^{-1}(y_d^{(n)} - \hat{f} - \dot{e}_c - K \operatorname{sign}(s)) \tag{6}$$

where y_d, e_c and $\operatorname{sign}(s)$ are vectors with y_{d_i}, e_{c_i} and $\operatorname{sign}(s_i)$ as components. This law gives

$$\dot{s} = -(I + E)K \operatorname{sign}(s) + \varepsilon_c$$

with error matrix E and vector ε_c, given by

$$E = \Delta B \hat{B}^{-1}; \quad \varepsilon_c = \Delta f + E(y_d^{(n)} - \hat{f} - \dot{e}_c)$$

From the known bounds on the components of ΔB and Δf, bounds β and α on the components of E and ε_c can be determined, such that

$$|E_{ij}(x^*)| \leqslant \beta_{ij}(x^*), \quad |\varepsilon_{c_i}(x^*, t)| \leqslant \alpha_i(x^*, t) \quad \text{for } i, j = 1, \ldots, m \tag{7}$$

Using the Lyapunov function candidate $V = \frac{1}{2} s^T s$, it is seen that all trajectories are directed towards the sliding surface $s = 0$ if $\dot{V} = s^T \dot{s} < 0$ for all $s \neq 0$. Hence, the gain K in the control law must satisfy

$$-s^T(I + E)K \operatorname{sign}(s) + s^T \varepsilon_c < 0 \quad \text{if } s \neq 0$$

Only diagonal matrices $K = \text{diag}(k)$ with $k = [k_1 \cdots k_m]^T$ are considered in the sequel. The condition is then implied by

$$\sum_{i=1}^{m} |s_i| \left(k_i + \text{sign}(s_i) \left(\sum_{j=1}^{m} E_{ij} \text{sign}(s_j) k_j - \varepsilon_{c_i} \right) \right) > 0 \quad \text{if } s \neq 0 \tag{8}$$

For simplicity it is assumed that the error bounds β and α in (7) are independent. Then (8) will hold if

$$|s|^T((I - P)k - \alpha) > 0 \quad \text{if } s \neq 0 \tag{9}$$

where $|s|$ is a vector with $|s_i|$ as components and P a matrix with components

$$P_{ij} = \begin{cases} \beta_{ij} & \text{if } s_i \neq 0 \wedge s_j \neq 0 \\ 0 & \text{otherwise} \end{cases} \tag{10}$$

It is tacitly assumed that $I - P > 0$.

The control law (6) is discontinuous across the sliding surface, resulting in chattering, excitation of unmodelled dynamics and high-frequency control activity. A comparison of some methods to avoid chattering can be found in De Jager.[6] One possibility to replace the sign function in (6) by the saturation function $\text{sat}(s, \Phi)$, where $\Phi = \text{diag}(\varphi) > 0$ with $\varphi = [\varphi_1 \cdots \varphi_m]^T$:

$$\text{sat}(s, \Phi)_i = \text{sat}(s_i, \varphi_i) = \begin{cases} \text{sign}(s_i) & \text{if } |s_i| > \varphi_i \\ s_i/\varphi_i & \text{if } |s_i| \leq \varphi_i \end{cases}$$

The domain in state space where $|s| \leq \varphi$ (i.e., where $|s_i| \leq \varphi_i$ for $i = 1, \ldots, m$) is called the boundary layer. The modified control law

$$u = \hat{B}^{-1}(y_d^{(n)} - \hat{f} - \dot{e}_c - K \text{sat}(s, \Phi))$$

guarantees attractiveness of this layer, but not of the sliding surface. The 's-dynamics' inside the boundary layer is now

$$\dot{s} + (I + E)K\Phi^{-1}s = \varepsilon_c \tag{11}$$

In practice, the controller is implemented as a sampled data one with finite sampling frequency $f_s = 1/\Delta t$. Then the components of φ must be lower bounded to keep s in the boundary layer. This will be the case if $|s(t)| \leq \varphi$ implies $|s(t + \Delta t)| \leq \varphi$. Forward Euler discretization of (11) to approximate $s(t + \Delta t)$ results, after some elaboration, in

$$(I - P)k - \alpha \geq 0 \wedge \frac{\Delta t}{2}(I + P)k + \alpha) \leq \varphi$$

The first inequality is satisfied if k satisfies

$$(I - P)k = \alpha + \kappa_c; \quad \kappa_c > 0$$

Obviously, then condition (9) is also satisfied. The second inequality then yields

$$\varphi \geq \Delta t (k - \tfrac{1}{2}k_c) \tag{12}$$

To avoid excitation of unmodelled dynamics, one sets the bandwidth of the error dynamics (5) lower than the lowest unmodelled resonant mode. This is achieved by a proper choice of the coefficients $\eta_{i,j}$ in (5). Also, one tries to set φ close to the bound in (12) to realize satisfactory tracking accuracy.

4. DYNAMICAL SLIDING MODE CONTROL

Recently, a new method has been proposed to circumvent chattering and, at the same time, retain the robustness of the ideal SMC.[3,4] The idea is to create a dynamical controller that eliminates the chattering problem by passing discontinuous actions onto a derivative of the input u.

As before, the first step is to introduce m switching co-ordinates s_i, now defined by

$$s_i = e_i^{(n_i)} + e_{d_i}; \quad e_i = y_i - y_{d_i}; \quad e_{d_i} = \sum_{j=1}^{n_i} \eta_{i,j} e_i^{(j-1)} \quad \text{for } i = 1, \dots, m \tag{13}$$

where the constants $\eta_{i,1}, \dots, \eta_{i,n_i}$ must guarantee the desired error dynamics if $s_i = 0$. With the usual definitions for s and e_d this results in

$$s = y^{(n)} - y_d^{(n)} + e_d = Bu - (y_d^{(n)} - f - e_d)$$

where (4) is used to eliminate $y^{(n)}$. Compared with (5), the order of the error dynamics is increased by one and now $y^{(n)}$ must be known to compute s. Bartolini,[3] and Bartolini and Pydynowski[5] showed that the attractiveness of the sliding surface $s = 0$ can still be guaranteed if $y^{(n)}$ is replaced by a suitable estimate $\hat{y}^{(n)}$ which converges to $y^{(n)}$.

The proposed dynamical control law is

$$\frac{\mathrm{d}}{\mathrm{d}t}(\hat{B}u) = y_d^{(n+1)} - \dot{\hat{f}} - \dot{e}_d - (K\,\mathrm{sign}(s) + L\,\mathrm{sat}(s, \Phi))$$

The reason for introducing the term $L\,\mathrm{sat}(s, \Phi)$ will be discussed later. Using this law yields

$$\dot{s} = -(I + E)(K\,\mathrm{sign}(s) + L\,\mathrm{sat}(s, \Phi)) + \varepsilon_d + \dot{E}\hat{B}u \tag{14}$$

where $E = \Delta B \hat{B}^{-1}$ is as defined before and the error vector ε_d is

$$\varepsilon_d = \Delta\dot{f} + E(y_d^{(n+1)} - \dot{\hat{f}} - \dot{e}_d) \tag{15}$$

In the previous section, bounds for the components of E were introduced. Now it is assumed that bounds for the components of $\dot{E}\hat{B}$ and ε_d can also be determined, i.e.,

$$|(\dot{E}\hat{B})_{ij}| \leqslant v_{ij}, \quad |\varepsilon_{d_i}| \leqslant \mu_i \quad \text{for } i, j = 1, \dots, m \tag{16}$$

To determine gain matrices K and L that guarantee the attractiveness of the sliding surface the same Lyapunov function candidate $V = \frac{1}{2}s^{\mathrm{T}}s$ as before is used. The condition $\dot{V} < 0$ if $s \neq 0$ now implies that K and L have to satisfy

$$-s^{\mathrm{T}}(I + E)(K\,\mathrm{sign}(s) + L\,\mathrm{sat}(s, \Phi)) + s^{\mathrm{T}}(\varepsilon_d + \dot{E}\hat{B}u) < 0 \quad \text{if } s \neq 0$$

For diagonal $K = \mathrm{diag}(k)$ and $L = \mathrm{diag}(l)$ this is true if

$$|s|^{\mathrm{T}}((I - P)(k + L\,\mathrm{sat}(|s|, \Phi)) - \mu - N|u|) > 0 \quad \text{if } s \neq 0 \tag{17}$$

with P defined by (10) and N the matrix with the bounds v_{ij} $(i, j = 1, \dots, m)$ as components. Contrary to the situation for the CSMC, the input u is also present.

Suppose that it is possible to find gains k and l that satisfy this inequality. Then, if switching of $\dot{u}$ is infinitely fast, s will remain zero from the moment the sliding surface is reached and, according to (13), perfect tracking is asymptotically achieved. In practice, however, switching is not infinitely fast, since the sampling frequency $f_s = 1/\Delta t$ is upper bounded. Suppose that $|s(t)| \leqslant \varphi$ for all $t > t_s$. Then the discretization of (14) inside the layer $|s| \leqslant \varphi$ yields

$$s(t + \Delta t) = s - \Delta t((I + E)(K\,\mathrm{sign}(s) + L\Phi^{-1}s) - \varepsilon_d - \dot{E}\hat{B}u)$$

where all time-dependent quantities on the right-hand side have to be taken at time t. If the term $L\Phi^{-1}s$ is omitted then, in general, the mean of s does not converge to zero, even in the situation without system uncertainties. Therefore, this term is required to force the *mean* of s in a sampled data implementation to zero. Of course, $L\Phi^{-1}$ must be large enough to be effective. However, to avoid instability, the gains in $L = \text{diag}(l)$ may not be too large.

To guarantee that s remains in this layer, $|s(t)| \leqslant \varphi$ must imply $|s(t + \Delta t)| \leqslant \varphi$ for all possible errors E, $\dot{E}\hat{B}$ and ε_d. It can be shown that this will be the case if $K = \text{diag}(k)$ and $L = \text{diag}(l)$ satisfy

$$(I - P)(k + l) - (\mu + N|u|) \geqslant 0 \wedge \frac{\Delta t}{2}((I + P)(k + l) + (\mu + N|u|)) \leqslant \varphi$$

The first inequality is satisfied if k and l satisfy

$$(I - P)(k + l) = \mu + N|u| + \kappa_d; \quad \kappa_d > 0$$

and then condition (17) is also satisfied. The second inequality then yields

$$\varphi \geqslant \Delta t(k + l - \tfrac{1}{2}\kappa_d) \tag{18}$$

With a sampled data controller implementation, perfect tracking cannot be achieved anymore. Besides, in practice, s will contain high-frequency components, due to unmodelled dynamics. Therefore, the bandwidth of the error dynamics in (13) is chosen lower than the lowest unmodelled resonant mode. For the DSMC this filtering can be more effective as a result of the higher order error dynamics. Again, it is best to set φ close to its bound.

In both approaches, the tracking accuracy δ_i is determined by φ_i and coefficient $\eta_{i,1}$ in the definition of s_i. The parameters φ_i are lower bounded by the magnitude of the modelling errors and the sampling frequency f_s. For a given system, the guaranteed tracking accuracy is thus limited by f_s.

5. EXPERIMENTS

To investigate the CSMC and DSMC in an experimental environment, they were implemented as sampled data controllers on a mechanical system (see De Jager and Banens[7] for a detailed discussion on the control system). The sampling frequency f_s was 200 Hz during all experiments. Unmodelled dynamics was, amongst other things, due to neglected joint flexibility. To study robustness and performance of the controllers, experiments were performed with two different trajectories.

5.1. System description

The system considered, an XY-table, is a big plotter-like machine moving in the horizontal plane, see Figure 1. Two parallel slideways each support a slide. These slides are connected with belts to a flexible spindle, which is driven by the x-motor. A third slideway rests on these slides and supports the end-effector, which is belt-driven by the y-motor. By replacing a thin strip in the spindle, the torsion stiffness of the spindle can be changed. Coulomb and viscous friction appear in all slides. Two encoder wheels on the motor shafts provide information on the position of the end-effector in the x-direction (y_1, resolution: $3.52 \, \mu$m) and the y-direction (y_2, resolution: $16.3 \, \mu$m). The system is controlled via the two motors.
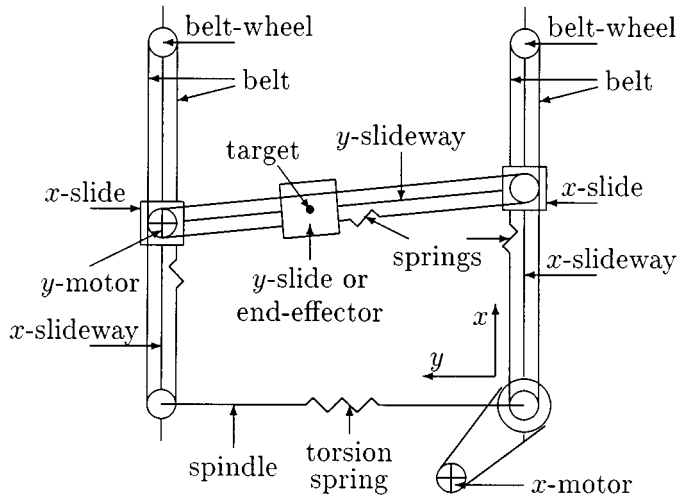
Figure 1. XY-table

Table I. Model parameters

Parameter	Value	Unit
a_1	34	kg
a_2	2·3	kg
a_3	40	N
a_4	13	N
a_5	35	Ns/m
a_6	5	Ns/m

If the flexible spindle is replaced by a rigid bar, the mathematical description of the XY-table yields the two degrees-of-freedom design model

$$a_1 \ddot{y}_1 + a_3 \operatorname{sign}(\dot{y}_1) + a_5 \dot{y}_1 = u_1$$
$$a_2 \ddot{y}_2 + a_4 \operatorname{sign}(\dot{y}_2) + a_6 \dot{y}_2 = u_2 \qquad (19)$$

Here, a_1 and a_2 are masses, $a_3 \operatorname{sign}(\dot{y}_1)$ and $a_4 \operatorname{sign}(\dot{y}_2)$ represent Coulomb friction, and $a_5 \dot{y}_1$ and $a_6 \dot{y}_2$ account for viscous damping, Finally, u_1 and u_2 are the generalized forces, exerted by the servomotors. The parameters a_1–a_6, identified by experiments, are listed in Table I.

The design model's order $n = 4$ equals its relative degree $r = 2 + 2$. In the notation of Section 2, it is

$$y^{(n)} = \hat{f}(x) + \hat{B}(x)u \qquad (20)$$

where $x = [y_1 \ \dot{y}_1 \ y_2 \ \dot{y}_2]^{\mathrm{T}}$, $u = [u_1 \ u_2]^{\mathrm{T}}$, $y^{(n)} = [\ddot{y}_1 \ \ddot{y}_2]^{\mathrm{T}}$, and

$$\hat{f}(x) = \begin{bmatrix} -(a_3 \operatorname{sign}(x_2) + a_5 x_2)/a_1 \\ -(a_4 \operatorname{sign}(x_4) + a_6 x_4)/a_2 \end{bmatrix}, \qquad \hat{B}(x) = \begin{bmatrix} 1/a_1 & 0 \\ 0 & 1/a_2 \end{bmatrix}$$

The most important sources of modelling errors are

- *Neglected flexibilities*: the spindle is assumed to be rigid and so are the springs used to attach the slides to the belts. This implies that the relative degrees of the real system and the design model are the same, but that the real system's order $n^* \geqslant 12$ is higher than the design model's order $n = 4$. Thus, unmodelled dynamics shows up in the internal dynamics of the real system.
- *Unmodelled friction components*: as a result of imperfections in bearings and shafts, there is a harmonic disturbance force (friction) in both the x-direction and the y-direction.
- *Parameter errors*: wrongly identified mass and friction parameters, the latter of which vary due to changing operating conditions.

It is impossible to give an *exact* description of the real system, as f and B are not available. However, estimates for f and B have been derived (see, e.g., Blom[8] and Van de Wal[9] from which estimates for Δf and ΔB can be obtained and used for controller design.

5.2. Controller and observer settings

The design and tuning of the controller parameters were based on simulations and experiments. Simulations were used for practical reasons: easy access to all variables of interest, gradual introduction of model errors, easy manipulation of system characteristics, etc.

For the design model, the switching co-ordinates s_i, $i = 1, 2$, are defined by

$$\text{CSMC: } s_i = \dot{e}_i + \eta_{i,1} e_i$$

$$\text{DSMC: } s_i = \ddot{e}_i + \eta_{i,2} \dot{e}_i + \eta_{i,1} e_i$$

As mentioned in Sections 3 and 4, the poles (and therefore the bandwidth) of the error dynamics should be chosen to filter unmodelled dynamics. The poles for $i = 1$, i.e., for the error in the x-direction, were placed at -12 rad/s, which corresponds to about half the expected resonance frequency of the lowest unmodelled mode for the XY-table with spindle stiffness 1·3 Nm/rad. The poles for $i = 2$, i.e., for the error in the y-direction, were placed at -30 rad/s to take into account that, for the y-direction, the resonance frequency of unmodelled modes which have a significant contribution in that direction is much higher than for the x-direction. This choice for the poles results in the coefficients $\eta_{i,j}$ of Table II.

Table II. Controller settings for experiments

| Parameter | CSMC | | | DSMC | | |
	x-direction ($i = 1$)	y-direction ($i = 1$)	Unit	x-direction ($i = 1$)	y-direction ($i = 1$)	Unit
$\eta_{i,1}$	12	30	rad/s	144	900	rad/s^2
$\eta_{i,2}$	—	—		24	60	rad/s
k_i	6	6	m/s^2	70	100	m/s^3
l_i	—	—		7·5	10	m/s^3
φ_i	0·07	0·07	m/s	0·75	1·0	m/s^2

The controller gains $k_1 \geqslant 0$ and $k_2 \geqslant 0$ (and for the DSMC $l_1 \geqslant 0$ and $l_2 \geqslant 0$) must satisfy condition (9) for the CSMC and (17) for the DSMC. In the current investigation, it was decided to use *fixed* values for the gains, so the earlier given relations in terms of (possibly state-dependent and input-dependent) error bounds were not used. One option is to derive worst-case values for k_i and l_i based on knowledge of the maximum input and the model error bounds in (7) and (16). However, this would result in control effort that is much higher than strictly needed, i.e., the controller would be conservative. An approach which partly resolves this shortcoming is discussed next.

For the CSMC, the *individual* sliding conditions $\dot{V}_i = s_i \dot{s}_i < 0$ are (see also (8))

$$-|s_i|(1 + E_{ii})k_i - s_i \sum_{j \neq 1}^{m} E_{ij} k_j \operatorname{sign}(s_j) + \varepsilon_{c_i} s_i < 0$$

Employing the relation $-E_{ij} s_i \operatorname{sign}(s_j) \leqslant |E_{ij}| |s_i|$, it is sufficient, for the sliding conditions to be fulfilled, that

$$-(1 + E_{ii})k_i + \sum_{j \neq i}^{m} |E_{ij}|k_j + \varepsilon_{c_i} \operatorname{sign}(s_i) < 0 \qquad (21)$$

For the XY-table, the following explicit expression for k_1 and k_2 results in

$$\begin{bmatrix} k_1 \\ k_2 \end{bmatrix} > \Gamma^{-1} \begin{bmatrix} \varepsilon_{c_1} \operatorname{sign}(s_1) \\ \varepsilon_{c_2} \operatorname{sign}(s_2) \end{bmatrix}; \quad \Gamma = \begin{bmatrix} 1 + E_{11} & -|E_{12}| \\ -|E_{21}| & 1 + E_{22} \end{bmatrix} \qquad (22)$$

Rewriting (21) as (22) is justified if $|E_{ij}| < 1$ and $\det(\Gamma) > 0$, which applies under all circumstances that can be expected for this system. Simulations for a circle trajectory (see Section 5.3) are now performed with a more advanced *evaluation model* which, contrary to the design model (19), accounts for the flexibility of the spindle. Parameters k_1 and k_2 are set equal to the maximum of the absolute value of the right-hand side of (22), giving

$$\text{CSMC: } k_1 = 3; \quad k_2 = 0{\cdot}035 \, \text{m/s}^2$$

In the case of the DSMC, k_i's are determined in a similar way. Provided the values for l_i are small compared with those for k_i, the individual sliding conditions are met if

$$\begin{bmatrix} k_1 \\ k_2 \end{bmatrix} > \Gamma^{-1} \begin{bmatrix} (\varepsilon_{d_1} + \frac{\mathrm{d}}{\mathrm{d}t}(\Delta B_{11})u_1 + \frac{\mathrm{d}}{\mathrm{d}t}(\Delta B_{12})u_2)\operatorname{sign}(s_1) \\ (\varepsilon_{d_2} + \frac{\mathrm{d}}{\mathrm{d}t}(\Delta B_{21})u_1 + \frac{\mathrm{d}}{\mathrm{d}t}(\Delta B_{22})u_2)\operatorname{sign}(s_2) \end{bmatrix}$$

For the DSMC, the term $\Delta \dot{f}_i$ in ε_d may contain Dirac-functions if Coulomb friction is present. However, these effects last for a very short time and it is assumed that stability will not be endangered if they are neglected in the derivation of the gains k_i. Similar simulations as for the CSMC result in the following values:

$$\text{DSMC: } k_1 = 45; \quad k_2 = 1{\cdot}5 \, \text{m/s}^3$$

During the experiments, the sliding surface must be reached within 0·5 sec, starting from $(y_1, y_2) = (0{\cdot}5, 0{\cdot}5)$. To satisfy this requirement, the gains k_i have to be increased, while k_2 for the CSMC have to be tuned up even more due to modelling errors in the evaluation model. The final values used for the experiments are listed in Table II.

Controller parameters l_i are chosen such that the mean of s will rapidly converge to zero, without endangering stability. Parameters φ_i in Table II are determined according to the

directives in the previous sections, see (12) and (18), but φ_i for the CSMC need to be increased in the experimental environment to avoid unstable behaviour.

Since only the measured positions y_1 and y_2 are used for feedback, the velocities, and in case of the DSMC also the accelerations, are obtained by means of an observer. In order to compensate for the time delay Δt in the sampled data implementation, positions, velocities and accelerations are determined one-step-ahead. For the purpose of observer design, the discontinuous nonlinear Coulomb friction term $\hat{d}$ in $\hat{f}$ is absorbed into the input u':

$$y^{(n)} = \hat{f}'(x) + \hat{B}(x)u'; \quad \hat{f}'(x) = \hat{f}(x) - \hat{d}(x); \quad u = u' - \hat{B}^{-1}(x)\hat{d}(x)$$

with $\hat{f}'$ continuous and u the actually applied input. The observer was designed employing this relation instead of (20).

For the CSMC, the observer design is based on a Kalman-like approach. For this purpose, a discrete-time version of the state-space description for the XY-table (19) is used (the subscript 'd' denotes discrete time versions of the associated matrices):

$$\text{design model: } x(t + \Delta t) = A_d x(t) + B_d u'(x(t), t) \tag{23}$$

$$\text{'real' system: } x(t + \Delta t) = A_d x(t) + B_d u'(x(t), t) + w(t)$$

$$\text{measured positions: } y(t) = C_d x(t) + v(t)$$

where v represents measurement noise and w 'process noise' (modelling errors). In order to design a Kalman filter, the covariance matrices for v and for w are determined. For v, this is related to the quantization error of the position encoder wheels, that is known from the resolutions given before. The covariance of w is estimated by means of an experiment with the CSMC. After the experiment, the actual velocity and acceleration in $\dot{x}$ are approximated via a central difference scheme. Now w is determined from the difference between the required u' for the design model (23) to follow the 'measured' trajectory exactly and the measured u' for the real system. Given the covariance matrices, the gain L_d in the one-step-ahead observer

$$\hat{x}(t + \Delta t) = A_d \hat{x}(t) + L_d(y(t) - C_d \hat{x}(t)) + B_d u'(\hat{x}(t), t) \tag{24}$$

can be computed. However, to realize stable controlled system dynamics, L_d had to be detuned. This was achieved by computing the covariance after high-pass filtering of w with a cut-off frequency of 10 Hz, by which deterministic components in w are partially eliminated in the Kalman filter design. Another approach would be to increase the covariance of v. The ultimately resulting L_d is given below:

$$L_d = \begin{bmatrix} 2{\cdot}56 & 0 \\ 313 & 0 \\ 0 & 1{\cdot}40 \\ 0 & 120 \end{bmatrix}$$

The natural frequencies ω_n and natural damping factors ζ_n for the observer in the x-direction are $\omega_n = [120, 822]$ rad/s, $\zeta_n = [1{\cdot}00, 1{\cdot}00]$, and in the y-direction $\omega_n = [234, 234]$ rad/s, $\zeta_n = [0{\cdot}685, 0{\cdot}685]$.

Unfortunately, several efforts for a similar design of an observer which also estimates accelerations were not successful in the sense that the resulting closed-loop system was unstable. Instead, for the DSMC, the observer discussed above was extended with a Luenberger observer which provides acceleration estimates:

$$\hat{x}^*(t + \Delta t) = A_d \hat{x}^*(t) + L_d^*(y^*(t) - C_d \hat{x}^*(t)) + B_d \dot{u}'(\hat{x}(t), \hat{x}^*(t), t) \tag{25}$$

Here, $\hat{x}^* = \hat{x}$, $y^* = [\hat{x}_2 \; \hat{x}_4]^T$ contains the velocity estimates by the Kalman-like filter, and L_d^* is the gain for the Luenberger observer. It is emphasized that only the $\hat{\bar{y}}_i$'s in $\hat{x}^*$ are used for control. By choosing

$$L_d^* = \begin{bmatrix} 0.235 & 0 \\ 2.74 & 0 \\ 0 & 0.235 \\ 0 & 2.74 \end{bmatrix}$$

natural frequencies ω_n and natural damping factors ζ_n for the observer in the x-direction are $\omega_n = [26.0, 26.0]$ rad/s, $\zeta_n = [0.982, 0.982]$, and in the y-direction $\omega_n = [27.1, 27.1]$ rad/s, $\zeta_n = [0.962, 0.962]$. In the y-direction ω_n is close to the bandwidth aimed at by the control law.

5.3. *Experiments with circular trajectory*

During the first experiments, the desired trajectory was chosen to be a circle

$$y_{d_1} = 0.5 - 0.25\cos(2\pi f_e t) \text{ m}$$

$$y_{d_2} = 0.5 - 0.25\sin(2\pi f_e t) \text{ m}$$

with f_e successively fixed at 0.5 Hz and 0.25 Hz.

First, results of experiments with desired trajectory (26) and $f_e = 0.5$ Hz will be discussed. In Figure 2, upper plot, the results for the root mean square (RMS) of e_1, i.e., the tracking error in the x-direction, are plotted against the stiffness of the spindle. From this plot, it is concluded that the performance of both controller schemes is approximately the same for all considered stiffnesses. This also holds with respect to robustness, since the sensitivity to variations in the stiffness is about the same.

The same experiments were carried out with $f_e = 0.25$ Hz, see Figure 2 lower plot. Again robustness is approximately the same, but now the performance of the CSMC is always better than that of the DSMC. A sound explanation for this trajectory dependency has not yet been found. Van de Wal[9] mentioned the errors in the predicted states as possible causes.

For $f_e = 0.25$ Hz the error e_1 for both controller schemes is more affected by the value of the stiffness than for $f_e = 0.5$ Hz. Probably, the influence of other modelling errors, such as inertia and viscous damping parameter errors, is more dominant at higher speeds.

The influence of varying mass parameters on the performance can be investigated by mounting additional masses on the end-effector. During the experiments, it was observed that robustness to parameter errors is about the same for both controller schemes. However, the experimental results are poor: additional masses larger than about 50 per cent of the nominal mass cause instability, even after detuning η_{21} for the CSMC to 20 rad/s and for the DSMC to 400 rad/s². This is somewhat disappointing, since good control has been obtained for larger masses (see, e.g., Blom and De Jager[10]). The errors in the predicted states are believed to be the main reason for this.

Although not depicted, slight chattering with the DSMC occurs in both control inputs. This is due to the sampled data implementation and the finite sampling frequency f_s. Larger values for f_s are expected to reduce the chattering effects. Since, for the experimental set-up, the controller and observer parameters needed substantial retuning for sampling frequencies other than 200 Hz, this conjecture was only supported by simulations, for which the controller parameters could be maintained and where all variables of interest were available.
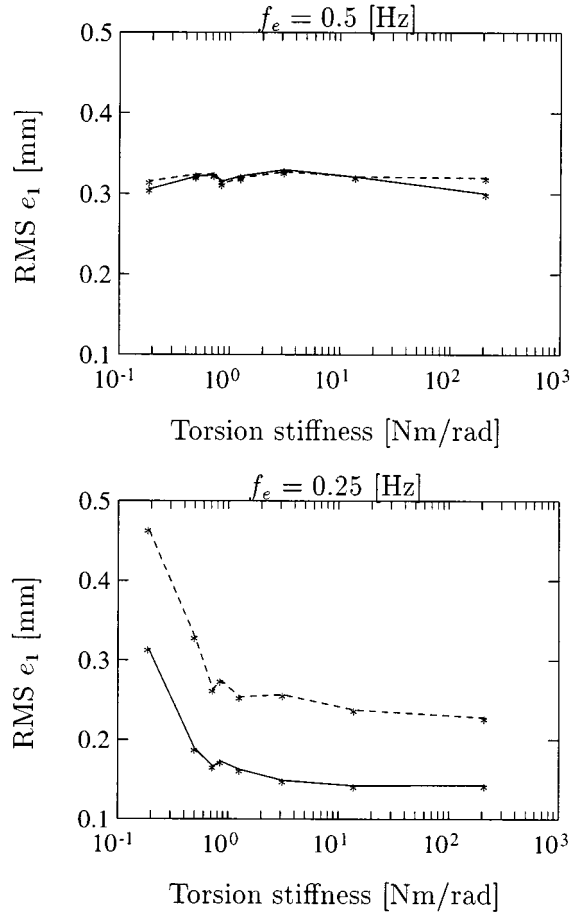
Figure 2. Robustness to unmodelled dynamics; solid: CSMC, dashed: DSMC

In addition, it is expected that the tracking error is strongly affected by f_s. Again, this has only been confirmed by simulations, which were performed for sampling frequencies between 200 Hz and 2 000 Hz. During all simulations, displacements, velocities and accelerations were 'measured', while one-step-ahead prediction was not necessary. Instead, the constant input applied in the interval $(t, t + \Delta t]$ was based on measurements obtained at t. The tracking errors tended to decrease for increasing f_s: for the DSMC in both directions and for the CSMC in the y-direction. In the x-direction, the error with the CSMC was approximately constant. For the range of sampling frequencies investigated, performance with the CSMC was always better than with the DSMC, but the difference was smaller for larger f_s.

5.4. Experiments for a torch burning task

In a second series of experiments, the performance of the controllers was studied with the XY-table performing a more specific industrial manufacturing task, such as torch burning. The
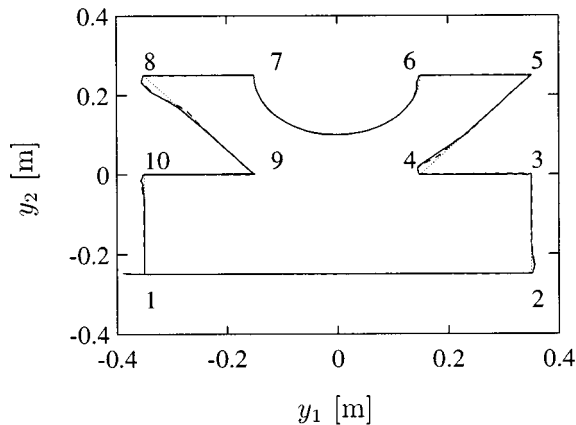
Figure 3. Desired and realized trajectories; dotted: desired; solid: CSMC; dashed: DSMC

trajectory consists of several parts (Figure 3), that have to be tracked at a constant speed of 0·3 m/s, starting to the left of the corner point 1. The effect of the Dirac-functions in the desired acceleration at the corner points are, to a certain extent, taken into account by temporarily prescribing the maximally realizable acceleration. This modification of the desired trajectory must last as many sample moments as it takes to realize the change in impulse of the system ('$a_1 \Delta \dot{y}_{d_1}$, $a_2 \Delta \dot{y}_{d_2}$') moving from one trajectory part to another.

   To avoid chattering of u due to incorrect Coulomb friction compensation, the computed torque part $\hat{f}$ in both the CSMC and the DSMC was slightly modified: the sign-function in the friction compensation part was replaced by a saturation function, thereby avoiding chattering in the input signals in trajectory parts with zero velocity in one direction.

   During the experiments, the DSMC settings from Table II were used, except for φ_2 which had to be set three times higher to guarantee that, after entering, s remained inside the boundary layer. The associated parameter l_2 was also set three times higher.

   Figure 3 shows the desired trajectory and the realized trajectories with a CSMC and a DSMC. In Figure 4, the tracking errors e_1 and e_2 are depicted. It is concluded that for e_1 the CSMC performs better than the DSMC. Note the overshoot with the DSMC after passing the fourth and eighth corner point.

   On trajectory parts with zero desired velocity in the y-direction, steady-state tracking errors in this direction occur with the CSMC. This is due to imperfect Coulomb friction compensation, implying persistent disturbances in the s-dynamics, which cannot be filtered out. With respect to the DSMC, this modelling error causes impulses (non-persistent disturbances) at the input of the s-dynamics, resulting in converging tracking errors (although convergence is slow in trajectory part 1–2).

6. CONCLUSIONS AND RECOMMENDATIONS

In this paper, a particular method to eliminate chattering in SMC is discussed. The fundamental idea is to introduce a first-order dynamical controller. However, owing to the finite sampling
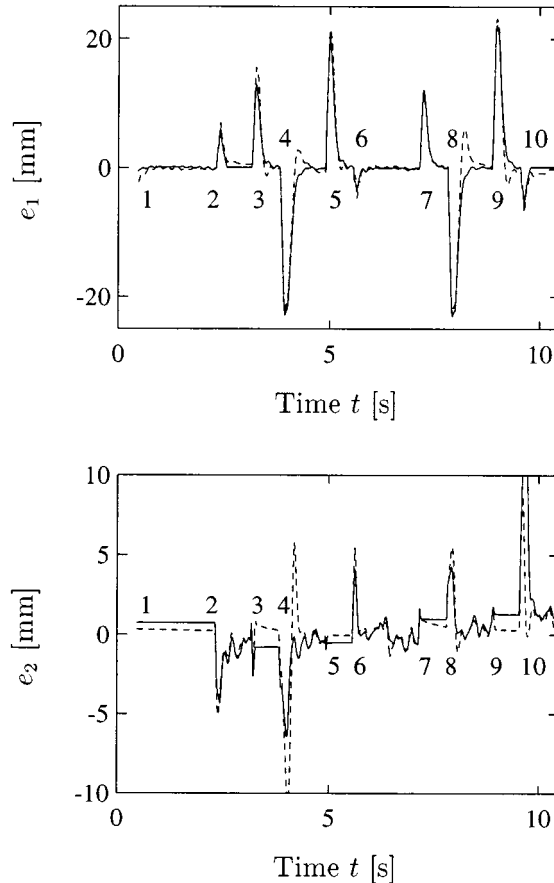
Figure 4. Tracking errors in x- and y-directions ('clipped'); solid: CSMC; dashed: DSMC

frequency f_s, slight chattering still occurs in a sampled data implementation. Larger values for f_s will diminish this.

Theoretically, stability and asymptotically perfect tracking for the DSMC can be achieved in the presence of modelling errors, provided that the errors are bounded with known bounds and that the gains in K are large enough. These gains depend on the system input, the system state and the desired trajectory. If physical bounds on the state and input are used to obtain K, this may result in a controller that is conservative. To avoid this, simulations with a more accurate evaluation model, or experiments, could be performed. Afterwards, the required gains could be computed from the 'modelling errors'. Since in robust control it should not be necessary to develop an extended model just to determine proper controller parameters, other methods to determine the controller gains are an important issue for future research. Spong[11] showed that for modelling errors due to uncertain inertia parameters, the uncertainty bounds needed for a specific controller, depend *only* on these parameters and *not* on the desired trajectory, the state or the control input. This is a desirable property, which is not shared by the controllers discussed in this paper.

To apply DSMC, the variables $y^{(n)}$ must be determined by measurement or by estimation. Combining DSMC with a robust observer deserves special attention in future research. Special attention has to be paid to the observer for the experimental system. The imperfect state estimates are believed to considerably influence the results.

Although the controllers are designed in continuous time, they are implemented as sampled data ones, thereby introducing discretization errors. Unfortunately, in such an implementation the perfect tracking property of the DSMC is lost, since the error dynamics is excited by a non-zero sliding vector s. Owing to this 'leak', the bandwidth of the error dynamics in the DSMC cannot be set arbitrarily high if excitation of high-frequency unmodelled dynamics has to be avoided. In a continuous implementation, s would be exactly zero and a high bandwidth of the error dynamics in the DSMC could be chosen to guarantee a fast response. So, owing to the sampled data implementation, an important advantage of the DSMC over the CSMC is eliminated. This may be the main reason that during the experiments the robustness of the DSMC to unmodelled dynamics is not better than that of the CSMC. It seems worthwhile to thoroughly trace the influence of discretization errors on the tracking performance and to develop versions of the DSMC directly targeted at sampled data systems.

REFERENCES

1. Utkin, V. I., 'Variable structure systems with sliding modes', *IEEE Trans. Automat. Control*, **AC–22**(2), 212–222 (1977).
2. Slotine, J.-J. E and W. Li, *Applied Nonlinear Control*, Prentice-Hall, Englewood Cliffs, New Jersey, 1991.
3. Bartolini, G., 'Chattering phenomena in discontinuous control system', *Int. J. Systems Sci.*, **20**, 2471–2481 (1989).
4. Sira-Ramírez, H., 'Dynamical sliding mode control strategies in the regulation of nonlinear chemical processes', *Int. J. Control*, **56**, 1–21 (1992).
5. Bartolini, G. and P. Pydynowski, 'Asymptotic linearization of uncertain nonlinear systems by means of continuous control', *Int. J. Robust Nonlinear Control*, **3**, 87–103 (1993).
6. De Jager, B., 'Comparison of methods to eliminate chattering and avoid steady state errors in sliding mode digital control', *Proceedings of the IEEE Workshop on Variable Structure and Lyapunov Control of Uncertain Dynamical Systems*, A. Zinober (Ed), Sheffield, UK, 1992, pp. 37–42.
7. De Jager, B. and J. Banens, 'Experimental evaluation of robot controllers, *Proceedings of the 33rd IEEE Conference on Decision and Control*, Vol. 1, Lake Buena Vista, FL, IEEE, Piscataway, NJ, pp. 363–368.
8. Blom, A., 'Robustness of a second order sliding mode controller', MSc thesis, Report WFW 93.007, Eindhoven University of Technology, Faculty of Mechanical Engineering, 1993.
9. Van de Wal, M., The slippery road to sliding control: evaluation of a dynamical sliding mode controller', MSc thesis, Report WFW 93.127, Eindhoven University of Technology, Faculty of Mechanical Engineering, 1993.
10. Blom, A. and A.G. de Jager, 'Robustness of a second order sliding mode controller', *Proceedings of the 1993 ASME Winter Annual Meeting*, E. A. Misawa (Ed), Vol. DSC-Vol. 53, New York, ASME, New Orleans, Louisiana, 1993, pp. 71–77.
11. Spong, M.W. 'On the robust control of robot manipulators', *IEEE Trans. Automat. Control*, **37**(11), 1782–1786 (1992).